

KAON PRODUCTION AT LARGE SPACE-LIKE MOMENTUM TRANSFER

O.K. BAKER*

*Department of Physics, Hampton University, Hampton, VA 23668,
and Physics Division, Jefferson Lab, Newport News, VA 23606
E-mail: baker@jlab.org*

The $^1\text{H}(e, e'K^+)\Lambda$ reaction was studied as a function of squared four-momentum transfer, Q^2 , between 0.52 and 2.00 $(\text{GeV}/c)^2$, and of the virtual photon polarization parameter, ϵ , with high precision. The experiment, E93018, was carried out in Hall C at Jefferson Lab in 1996. The results of the experiment show the need for revision of the some previous models of kaon electroproduction in this kinematic regime.

1 Introduction

One of the challenges faced in the study of hadronic systems with strangeness is getting a good understanding of the elementary amplitudes in kaon electroproduction. This is, in principle, possible now with the new high intensity, CW electron beam at Jefferson Lab. The electromagnetic production of strangeness via the $(e, e'K)$ reaction provides new and complementary information to that from hadronic reactions^{1,2} such as (K, π) , (π, K) and $(p, p'K)$ ⁵. This information is useful in such studies as hypernuclear production and spectroscopy, some aspects of QCD model building³ such as the basic coupling constants needed in nucleon-meson and quark models, and conjectured strange star⁴ behavior, to name only a few.

Experiment E93018 at Jefferson Lab was a high precision measurement of the longitudinal and transverse cross sections in the reaction $e + p \rightarrow e' + K^+ + Y$ where Y is the associated hyperon, in this case a Λ or Σ hyperon. The experiment was designed to measure the separated components of the center of mass cross sections over a range of space-like momentum transfers. This motivated more detailed comparison to model calculations.

For this electroproduction experiment, the incident ($e = (E, \vec{p}_e)$) and scattered ($e' = (E_{e'}, \vec{p}_{e'})$) electrons define the scattering plane. The recoiling K^+ meson ($k = (E_K, \vec{p}_K)$) and the associated hyperon Y ($Y = E_Y, \vec{p}_Y$) define the production plane. The target proton is characterized by $p = (m_p, \vec{0})$ (that is, there is no momentum for the target proton in the the laboratory frame). The virtual photon lies in both planes. The angle between the electron scattering

*FOR THE E93018 COLLABORATION.

plane and the production plane is denoted by ϕ . The polar angle between the virtual photon and the kaon is denoted by $\theta_{\gamma K}$ while the angle between the incident and scattered electron is θ_e . The four-momentum transfer from the electron to the proton is $q (= e - e')$. Its components are $E - E_e' = \nu$ (the energy loss in the laboratory system) and $\vec{q} = \vec{p}_e - \vec{p}_{e'}$. The square of the four momentum transfer $q^2 = -Q^2$ is sometimes referred to as the mass of the virtual photon. Neglecting the mass of the electron (valid at these high energies), one can write $q^2 = -4EE'\sin^2(\theta_e/2)$. Other quantities of interest are $W^2 = m_p^2 + 2m_p\nu - Q^2$, the mass squared of the system recoiling against the electron, and the Mandelstam variables $t = (q - k)^2 = q^2 + m_K^2 - 2\vec{q} \cdot \vec{k}$, $s = (e + p)^2 = m_p^2 + 2m_pE$ and $u = (k - p)^2$.

In the one-photon-exchange approximation (valid for this measurement), the differential cross section for an unpolarized electron scattering from an unpolarized target where the kaon is detected in coincidence with the scattered electron and no final state polarizations are detected, may be written as⁶

$$\frac{d^5\sigma}{dE'd\Omega_{e'}d\Omega_{K^+}} = \Gamma(\sigma_T + \epsilon\sigma_L + \epsilon\cos(2\phi)\sigma_{TT} + [\frac{\epsilon(\epsilon+1)}{2}]^{1/2}\cos\phi\sigma_{LT}) \quad (1)$$

where

$$\Gamma = \frac{\alpha}{4\pi^2} \frac{E_{e'}(W^2 - m_p^2)}{Em_pQ^2(1 - \epsilon)} \quad (2)$$

is the virtual photon flux. σ_T is the unpolarized (transverse) cross section, σ_L is the longitudinal cross section, σ_{TT} and σ_{LT} are the transverse-transverse and longitudinal-transverse interference cross sections. $d\Omega_{e'}$ and $d\Omega_{K^+}$ are the solid angles for electron and kaon detection, respectively. The cross sections completely characterize the hadronic system. In general, these cross sections are functions of Q^2 , W , and t . The last two terms in (2) vanish in parallel kinematics. Then by measuring the cross section at several values of ϵ while holding Q^2 , W , and t constant, the longitudinal and transverse cross sections may be determined separately. Jefferson Lab Experiment E93-018 was the very first experiment to accurately determine these cross sections. The central kinematics can be found in Niculescu⁷.

The use of the detector packages in both the electron (Hall C High Momentum Spectrometer) and hadron (Short Orbit Spectrometer) arms yielded a clean separation of the electron kaon coincidence events. Using the resulting formula for the cross section in parallel kinematics, all of the ϵ points for a given Q^2 were then fit to a straight line using linear least-squared fitting. The results of these fits are shown in Figure (1).

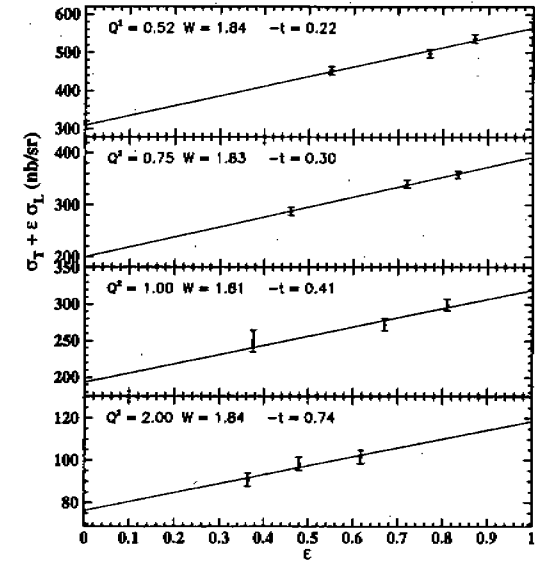


Figure 1. The linear least squares fit to the ϵ dependence of the total cross section. The slope of the line give σ_L while the intercept gives σ_T .

2 Results and Discussion

From the slopes and intercepts of the curves in Figure 1 the longitudinal and transverse cross sections may be extracted with good precision. The ratio of the longitudinal and transverse cross sections, R , is subsequently calculated and compared to model predictions. This ratio is shown in Figure 2, along with several calculations for comparison with the data. The medium thickness dashed curves correspond to the calculations by the Saclay-Lyon (SL) group⁸ using an isoabarc model for the transition form factors. The medium thickness solid curves correspond to older calculations by Williams, Ji, and Cotanch⁹ (WJC) also using an isobaric model while the dot-dash curve correspond to more recent calculations⁹. The thin dashed curves correspond to newer calculations by Bennhold, Mart, and Hyde-Wright, also based upon an isobaric model. The thicker weight curves correspond to a Regge model calculation of Vanderhaeghen, Guidal, and Laget¹⁰ (VGL). From these curves, one can also extract a (rather model dependent) kaon form factor. This latter study is presently continuing as the data from the Σ hyperon are being analyzed.

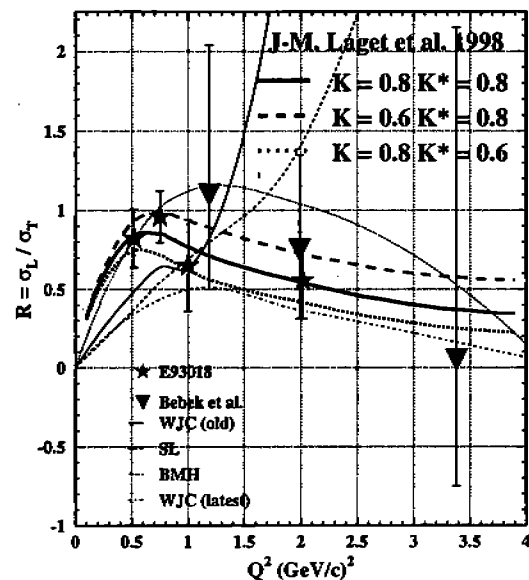


Figure 2. The ratio of the longitudinal to the transverse cross section for kaon electroproduction. The thin curves correspond to calculations of the Saclay-Lyon group, the medium thickness curves correspond to the calculations by Williams, Ji, and Cotanch, and the thicker lines show the calculations of Vandergaegen, Guidal, and Laget as discussed in the text.

As can be seen, the older SL model shows a steep rise in R vs Q^2 dependence (after the initial rise from $Q^2=0$ predicted by all models), in contrast with the behavior exhibited by the data which is rather flat with increasing Q^2 . The older WJC calculation shows a pronounced rise of the ratio initially as well, although newer calculations show more agreement with the flat momentum transfer dependence. The VGL model shows a similar squared four-momentum transfer dependence as the newer WJC model and the data for the ratio R .

The main differences between the two isobaric model calculations (SL⁸ and WJC⁹) is that the former includes resonances up to spin 5/2 whereas the latter includes only up to spin 3/2 hadronic resonances. This difference would show up in a more striking manner in the transverse cross section since it is expected that higher mass and higher spin resonances (kaon and hyperon) couple more strongly to the transverse virtual photons in the forward direction. In the longitudinal channel, the cross section is expected to be dominated by

the t -channel kaon exchange, and not as sensitive (by comparison with the transverse channel) to s and u channel exchanges. The VGL Regge model calculation includes all resonances lying on the appropriate hadron trajectory¹⁰. This particular model provides a rather good description of the Q^2 dependence of R , showing the utility of the Regge description of kaon electroproduction processes. It is also intriguing to speculate that the inclusion of even higher spin/mass resonances, or even hidden resonances (which would decay strongly into a kaon and lower mass hyperon) would provide an even better description of the Q^2 dependences of these kaon electroproduction cross sections^{7,11}. In the near future, the analysis of the Σ channel will be completed and compared with models calculations.

Acknowledgments

This work is supported by the Department of Energy Award DE-FG02-97ER41035.

References

1. C. Bennhold, *Nucl. Phys. A* **547**, 79c (1992); Z. Li, *Phys. Rev. C* **52**, 1648 (1995).
2. C. Bennhold and L.E. Wright, *Phys. Rev. C* **36**, 438 (1987); S.R. Cotanch and S.S. Hsio, *Nucl. Phys. A* **450**, 419c (1986).
3. R.A. Schumacher, *Nucl. Phys. A* **585**, 63c (1995).
4. X.-D. Li *et. al.*, *Phys. Rev. Lett.* **83**, 3776 (1999).
5. R.A. Williams, C.R. Ji, and S.R. Cotanch, *Phys. Rev. C* **46**, 1617 (1992).
6. R.C.E. Devenish and D.H. Lyth, *Phys. Rev. D* **5**, 47 (1972).
7. G. Niculescu, Ph.D. Dissertation, Hampton University (unpublished), (1998).
8. J.C. David *et. al.*, *Phys. Rev. C* **53**, 2613 (1996).
9. R.A. Williams, private communications (1998).
10. M. Guidal, J.M. Laget, and M. Vanderhaeghen, *Phys. Lett. B* **400**, 6 (1997); *Nucl. Phys. A* **627**, 645 (1997); M. Vanderhaeghen, M. Guidal, and J.M. Laget, *Phys. Rev. C* **57**, 1454 (1998).
11. C. Bennhold, private communications (2000).